World Academy of Science, Engineering and Technology
International Journal of Mechanical and Mechatronics Engineering
Vol:11, No:6, 2017

Heat Transfer Dependent Vortex Shedding of Thermo-Viscous Shear-Thinning Fluids

Markus Rütten, Olaf Wünsch

***Abstract*—**Non-Newtonian fluid properties can change the flow behaviour significantly, its prediction is more difficult when thermal effects come into play. Hence, the focal point of this work is the wake flow behind a heated circular cylinder in the laminar vortex shedding regime for thermo-viscous shear thinning fluids. In the case of isothermal flows of Newtonian fluids the vortex shedding regime is characterised by a distinct Reynolds number and an associated Strouhal number. In the case of thermo-viscous shear thinning fluids the flow regime can significantly change in dependence of the temperature of the viscous wall of the cylinder. The Reynolds number alters locally and, consequentially, the Strouhal number globally. In the present CFD study the temperature dependence of the Reynolds and Strouhal number is investigated for the flow of a Carreau fluid around a heated cylinder. The temperature dependence of the fluid viscosity has been modelled by applying the standard Williams-Landel-Ferry (WLF) equation. In the present simulation campaign thermal boundary conditions have been varied over a wide range in order to derive a relation between dimensionless heat transfer, Reynolds and Strouhal number. Together with the shear thinning due to the high shear rates close to the cylinder wall this leads to a significant decrease of viscosity of three orders of magnitude in the nearfield of the cylinder and a reduction of two orders of magnitude in the wake field. Yet the shear thinning effect is able to change the flow topology: a complex Kármán vortex street occurs, also revealing distinct characteristic frequencies associated with the dominant and sub-dominant vortices. Heating up the cylinder wall leads to a delayed flow separation and narrower wake flow, giving lesser space for the sequence of counter-rotating vortices. This spatial limitation does not only reduce the amplitude of the oscillating wake flow it also shifts the dominant frequency to higher frequencies, furthermore it damps higher harmonics. Eventually the locally heated wake flow smears out. Eventually, the CFD simulation results of the systematically varied thermal flow parameter study have been used to describe a relation for the main characteristic order parameters.

***Keywords*—**Heat transfer, thermo-viscous fluids, shear thinning, vortex shedding.

I. Introduction

NON-NEWTONIAN fluids reveal a wide variety of properties due to their non-linear behaviour of viscosity in shearing flows. Since these types of fluids are widely used in technical, industrial, medical and also biological applications the knowledge about their complex properties and flow behaviour is necessary for the design of novel devices. The complex flow behaviour is caused by their molecular composition. Long entangled molecular chains lead to higher viscosities. High shear flow rates can tighten and align the molecular chains which leads to an decrease of the shear viscosity. The flow effects of those processes are not easily to predict, in particular in complex flow applications [3], [5].

The flow prediction is even more difficult when additional thermal loads are playing a significant role, since high molecular weight fluids are more sensitive to temperature influences on the viscosity [24]. Thus, heat transfer at walls and bluff bodies, its effect on the nonlinear viscosity and the resulting flow phenomena are a main focal point in the research field of non-Newtonian fluids [4], [6], [19], [11]. In particular, heat exchanger, lubrication systems or oil cooler are technical application in which the properties of non-Newtonian fluids are essential for the design and layout. Numerical simulations, conducted during the design process of such applications, are based on very accurately described fluid models [18]. Therefore, experimental and numerical studies are necessary to capture all phenomena which are related to thermal vicosity properties of non-Newtonian fluids.

In order to separate and to distinguish between different flow and thermal effects simple research configurations and setups are prefered. This paper concentrates on the flow around a cylinder and focuses on the wake flow behind a heated circular cylinder in the laminar vortex shedding regime. The phenomenon of vortex shedding from a bluff body is an interesting engineering and scientific problem. The so called Kármán vortex street [13], [14] is one of the most famous wake flows and commonly used as a classical test case for investigation of fluid properties. Mainly investigated for Newtonian fluids, it also reveals fluid properties of non-Newtonian fluids since the benefit of this cylinder flow are the high shearing rates, which have an significant effect on the shear dependent viscosity. This together with the geometric curvature of the cylinder results in a characteristical flow separation and a distinct vortex shedding. In this work from particular interest is the wake flow behind a heated circular cylinder in the laminar vortex shedding regime for thermo-viscous shear thinning fluids.

As shown by [13], [12], [16] the vortex shedding regime in the case of isothermal flows of Newtonian fluids, is characterised by a distinct Reynolds number and an associated Strouhal number. A lot of studies have been performed to derive relations also between the temperature and Strouhal - Reynolds number relation, see [22], [21] However, in the case of thermo-viscous shear thinning fluids the flow regime can more drastically change due to the further temperature impact at the viscous wall of the cylinder. The Reynolds number alters locally and, hence, the Strouhal number globally. A lot of experiments have been performe, but in most cases only higher Reynolds numbers ($Re > 40$) [9] have been considered. In case of creeping and low Reynolds number non-Newtonian

M. Rütten is with the German Aerospace Center (DLR), Institute of Aerodynamics and Flow Technology, 37073 Göttingen, Germany (e-mail: markus.ruetten@dlr.de).

O. Wünsch is with the University of Kassel, Dept. of Mechanical Engineering, Institute of Fluid Mechanics, 34125 Kassel, Germany (e-mail: wuensch@uni-kassel.de).

flows often steady flow has been assumed and focal point have been drag and the extension of separation bubbles, even when thermal effects have been considered [20].

In the present CFD study the temperature dependence of the Reynolds and Strouhal number is investigated for the flow of a shear thinning Carreau fluid around a heated cylinder for the low Reaynolds number range of 26 to 52. In particular th thermal viscosity effects are investigated. The temperature dependence of the thermal viscosity has been modelled by applying the Williams-Landel-Ferry (WLF) equation. In this numerical simulation campaign thermal boundary conditions have been varied over a wide range in order to derive a relation between the dimensionless heat transfer, the Reynolds and Strouhal number. Together with the shear thinning properties of the fluid under high shear rates close to the cylinder wall this results in a significant decrease of viscosity of three orders of magnitude in the nearfield of the cylinder and a reduction of two orders of magnitude in the wake field. Eventually the shear thinning effect is able to change the flow topology: a complex Kármán vortex street occurs, also revealing distinct characteristic frequencies associated with the dominant and sub-dominant vortices. The main focal point of this study is to investigate the change of the vortex shedding flow structures behind the cylinder and to reveal new unexpected flow behaviour.

II. The Non-Newtonian Fluid and the Simulation Setup

In contrast to Newtonian fluids the fluid properties of non-Newtonian play a significantly more important role in associated flows due to their ability to change their viscosity over orders of magnitude in dependence of flow caused shear rates. Overlayed thermal loads due to heat transfer can enforce these flow structure determining quantity. The acurate modelling of the fluid properties of the considered shear-thinning fluid is crucial for the simulation campaign. This together with a suitable CFD grid and a strict numerical simulation strategy is a precondition for reliable simulation results.

A. Properties of the Non-Newtonian Carreau Fluid

In this study we concentrate on a specific class of a non-Newtonian fluids: shear-thinning fluids without any yield stress or temporal relaxation properties. The simplest type of the considered shear-thinning fluid is a Ostwald - de Waele fluid [17] whose viscosity is modelled by a power law, therefore, these fluid are also called power-law fluids. However flow models purely based on the power law have the limitation that they do not posses any lower and upper viscosity limit. This leads to modelling errors at very low and very high shear rates, calculated by $\dot{\gamma} = \sqrt{\frac{1}{2}\left[\mathbf{D}:\mathbf{D}\right]}$, then viscosity can achieve unrealistic values. Furthermore, in comparison to other fluid models during numerical simulations their convergence rates are more worse, in particular in flow regions, in which the second invariant, I_2, of the strain tensors, $\mathbf{D} = \frac{1}{2}\left(grad\vec{v} + grad\vec{v}^T\right)$, is small, i.e. as in nearly uniform flows. In contrast to the power-law fluid the Carreau fluid model [7] has the advantage to have both a constant zero viscosity and a constant infinite viscosity which reflects the properties of real fluids very well [3]. The flow curve of a Carreau fluid is calculated by using (1),

$$\eta = \eta_\infty + (\eta_0 - \eta_\infty)\left\{1 + (\lambda\dot{\gamma})^2\right\}^{\frac{n-1}{2}}, \tag{1}$$

in which n is the flow index, η_0 the lower limit or zero viscosity, η_∞ the upper limit or infinite viscosity and $\dot{\gamma}$ the generalized shear rate. The parameter λ controls the transition from the Newtonian to the non-Newtonian behaviour. This parameter can be determined by the characteristic stress τ_γ, at which the deformation behaviour of the fluid changes: $\lambda = \eta_0/\tau_\gamma$. In principle this time constant is the reciprocal value of the critical shear rate $\dot{\gamma}_c$, at which exceeding shear rates start to reduce the viscosity of the fluid. In this simulation study we have used the following fluid parameters: $n = 0.2$, $\lambda = 0.11/s$, $\eta_0 = 10Pas$, $\eta_\infty = 0.001Pas$. The associated flow curve is depicted in Fig. 1. The small values of the time constant and the flow index are consciously chosen in order to achieve a high sensitivity of the fluid viscosity even to lower shear rates, so that the viscosity can drop orders of magnitudes. This is not unphysical, since low-density polymers, silicone oils or synthetic engine oils reveal such properties.

Modelling thermal-viscosity is a research field of its own: As many fluid models as many temperature-viscosity models exist. In this work the temperature dependency of the viscosity is modelled by the so-called *William-Landel-Ferry equation*, in short *WLF-equation*. This equation is used to determine the viscosity-temperature shift factor a_T, also called time-temperature superposition parameter, Andrade factor [1] or WLF shift factor [24], [11]. The WLF-equation reads as follows:

$$log\left(a_T\right) = log\left(\frac{\eta(\dot{\gamma}, T)}{\eta(\dot{\gamma}, T_{ref})}\right) = \frac{-C_1\left(T - T_{ref}\right)}{C_2 + \left(T - T_{ref}\right)}. \tag{2}$$

In this equation T_{ref} is the reference temperature, in this study a value of 403.15 K is assumed. The fluid parameters C_1 and C_2 have to be determind experimentally, for polymers the commonly used values are $C_1 = 8,86$ and $C_2 = 101,6K$, these values are taken in the simulation campaign.

Eventually the thermal-viscosity model has to be combined with the Carreau fluid model, this leads to the (3):

$$\eta\left(\dot{\gamma}, T\right) = a_T\eta_\infty + \frac{a_T(\eta_0 - \eta_\infty)}{1 + \left(a_T\lambda\dot{\gamma}\right)^{\frac{1-n}{2}}}, \tag{3}$$

which is implemented in the DLR Theta code for the simulation campaign.

B. Cylinder Flow Configuration and the Flow Solver

For the numerical simulation study a suitable flow domain with the cylindrical wall, the inflow, outflow and symmetry boundary conditions has to be generated. The flow domain is a two-dimensional rectangle which is in flow direction 18 times larger than the cylinder diameter D of 0.1 m, since the outer boundaries of the flow domain have to be far enough away from the cylinder to avoid reflecting effects on the cylinder and wake flow. The lower an upper symmetry wall have a distance

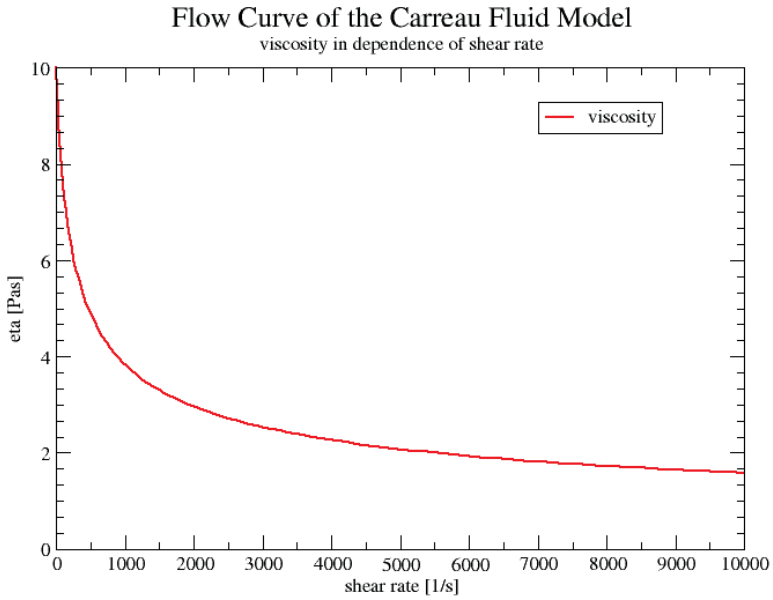

Fig. 1 Flow curve of the used Carreau fluid model, n = 0.2, $\lambda = 0.11/s$, $\eta_0 = 10Pas$, $\eta_\infty = 0.001Pas$

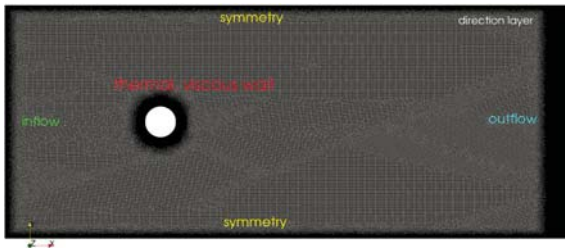

Fig. 2 Grid topology and boundary conditions

of 3.6 D to the cylinder wall, see Fig. 2, Numerical simulations of vortical flows are challenging. In particular special attention has to be paid to a very fine spatial grid resolution since vortex flow simulation and the associated analysing algorithms are often based on higher order derivatives. Thus, very smooth grid cell topologies and slow growing grid element aspect ratios are basic prerequisite for the used CFD grids. For the generation of the CFD grid the commercial mesher "Centaur" from the company CentaurSoft [2] has been applied. After some grid studies the CFD study has been conducted on a quasi two-dimensional hybrid grid consisting of prismatic and hexahedral elements and associated surface triangles and quadrilaterals. The corresponding purely two-dimensional grid consists of 140441 grid points, 229778 triangles and 21687 quadrilateral grid cells, last cells are stacked in 30 structured layers. This layer topology is necessary for resolving both the flow boundary and also the thermal boundary layer around the cylinder.

An impression of the grid topology is given in Fig. 2, also the assignment of the boundary conditions are shown. The cylinder wall is treated as thermal, viscous wall. In order to avoid artificial reflections at the symmetry and outflow boundaries the grid has been refined there.

The numerical simulations have been performed on a desktop computer using the DLR THETA code [15] for solving the incompressible Navier-Stokes equations. This code is a finite volume method based on the DLR standard flow solver TAU. A dual grid approach is applied to unstructured hybrid grids, all flow variables are stored at the same location, the so-called colocated respectively non-staggered grid approach. An efficient coupling of the velocity and the pressure fields is ensured by the projection method or the SIMPLE algorithm, see [23]. The well-known checkerboard instability of the pressure is eliminated by a 4th order stabilisation term, which is added to the left and the right hand side of the Poisson equation.

For spatial discretisation different upwind methods of 1st or 2nd to 3rd order as well as central 2nd order schemes can be used. Here a mixed second order scheme has been chosen combined with a special smoothing algorithm in order to get very smooth data for calculation of derived vector fields. A matrix-free formulation is used for solving the linear equations. This formulation reduces the memory requirements of the code considerably. A variety of multi-grid methods ensure efficient solutions of the linear equations, even on fine grids. Domain decomposition is used as a parallelization concept. The parallel efficiency is high on desktop computers with only a few CPUs as well as on massive parallel systems with hundreds of CPUs. The code is well validated by a variety of experimental and numerical validation campaigns and is state of the art in regard to performance, efficiency and accuracy [15]. In the considered flow case a $4-w$ multigrid cycle has been performed to accelerate the CFD calculations. The projection method has been used for the unsteady calculation, in which the timestep has been set to $0.001s$, resulting in grid cell CFL numbers less than one. The three point backward scheme, a variation of a BDF2 scheme, has been used for the temporal discretization.

In the present simulation campaign both the on-flow and thermal boundary conditions have been varied over a certain

range in order to derive a relation between dimensionless heat transfer, Reynolds and Strouhal number. At the inflow boundary a plug flow profile has been realised, its inflow velocity has been varied for 3 m/s to 6 m/s in 1 m/s steps. There, the inflow temperature has been specified to 403.15 K, at which the fluid has a density of $881\frac{kg}{m^3}$ and a zero viscosity of 10 Pas. Since the cylinder diameter of 0.1 m is used as reference length the initial Reynolds number varies from 26.43 for 3 m/s to 52.86 for 6 m/s. At the low Reynolds number flow condition a Newtonian fluid shows no vortex shedding, only a steady separation bubble. Beyond the critical Reynolds number of 40 the von Kármán vortex street can appear, the complexity of the flow dynamics increases [10], [25]. However, in case of non-Newtonian fluids with higher zero viscosity, flow separation and complex vortex shedding can occur earlier as reported in [9].

Additionally for each inflow velocity variation the temperature of the cylinder wall has increased stepwise from 405 K to 468 K in 5 K steps, whereas the temperature of the in-flowing fluid has kept constant at 403.15 K.

III. Analysis of the Simulation Results

At first the analyis of the simulation results starts with a FFT of cross velocity component fluctations which occur within the wake flow behind the cylinder. Thereto, a virtual sensor point has been placed behind the cylinder at the coordinates x = 0.025 m and y = 0.015 m, whereas the center point of the cylinder is taken as the origin of the coordinate system. During a simulation run at each time step the cross component of the velocity is stored into a file for further analyis.

In the second part of the analysis the flow topologies and vortex shedding pattern of the related flow cases which frequencies have been analysed before.

A. Frequency Analysis of the Vortex Shedding

In order to get an overview the FFT analysis starts with the flow around the unheated cylinder, which is the reference flow case with a global Reynold number of 26.43. In Fig. 3 a comparison of the frequence signature for the four onflow flow cases are depicted. As expected the shear-thinning property of the Carreau fluid leads to an earlier development of the Kármán vortex street like vortex shedding flow structure. The dominant frequencies are 7.8 Hz, 10 Hz, 11.8 Hz and 12.3 Hz. Obviously, with higher onflow velocities the significant energy rich dominant frequencies are shifted to higher values, though the dominant frequencies are becoming less pronounced with lower relative amplitudes. In case of 6 m/s onflow velocity the dominance of one alternating vortex structure is nearly lost.

Increasing the cylinder wall temperature to a value of 438 K has a significant consequence on the flow structure, which is indicated in Fig. 4. For both, the 3 m/s and 4 m/s flow cases, the vortex shedding has been nearly vanished. Only minor fluctations with a very low level of energy can be registered. In constrast for the higher onflow cases the dominance of one alternating vortex structure is enforcecd. Their dominant frequencies has nearly doubled to a value around 20 Hz. Remarkably the dominant frequency of the 5 m/s and 6m/S flow cases has changed the order, which means that the dominant frequency of the 5 m/s flow case is slighty higher than the corresponding of the 6 m/s flow case.

With further increasing of the cylinder wall temperature to 468 K the characteristical flow structures turn again. In Fig. 5 three aspects can be observed: At first, a vortex shedding related dominant frequency can be found again for the low onflow cases whilst in case of the the high onflow velocities the dominant frequencies are loosing their singnificance which is an indication for a decay of the main vortex shedding characteristic. Secondly, it has to be remarked that the amplitudes are very small in comparison to the former thermal flow cases. Thirdly, the dominant frequencies are shifted to lower values again when the vortex shedding is recovering.

Now we compare the results of the frequency analyis for the 4 m/s and 6 m/s onflow velocity cases over the whole range of the varied cylinder temperature. Figs. 6 and 7 only every second data curve is plotted in order to avoid too busy plots. The figures reveal global flow and vortex shedding characterists for both cases: At lower cylinder wall temperatures distinct dominant frequencies with their higher harmonics are eye-catching. With increasing temperature the dominant frequency is shifted to higher values but its amplitude is decreasing. At 438 K cylinder wall temperature the frequency analysis indicates that the vortex shedding process has nearly stopped, it can be assumed that only a separation bubble exists. With further higher temperatures the vortex shedding phenomena occurs again, the related frequencies are again lower than in the final state before the vortes shedding process stops. The related amplitudes are at least two to three orders of magnitude smaller.

To the highest temperature the frequencies are shifted again to higher values indicating an enforcement of the vortex shedding. Eventually, this can be called a weak vortex shedding regeneration process. The physical mechanisms behind this novel observation is not clear so far, thus further analyis is necessary.

Another interesting observations is depicted in Fig. 8. The Nusselt number is defined as the dimensionless heat flux, see (4),

$$Nu = \frac{\dot{q}}{T_W - T_\infty}\frac{D}{\lambda}, \tag{4}$$

whereas difference between the cylinder temperature and the inflow temperature is used for the normalisation. In this study we have extended the meaning of the characteristical number by comparison the inflow heat flux (zero) with the whole heat flux aleaving the flow domain at the outflow. This means that not only the heat transfer at the cylinder wall is considered but also the heat generated by dissipative effects in the flow field. The observation is the this last part is changing the balance, which means less vortex shedding has an important impact on the generation of heat due to dissipation. This aspect will be focus in future research work.

In Fig. 9 the Strouhal number dependency to the global Reynolds number and the cylinder wall temperature is shown. It is obvious that in case of the three lower Reynolds numbers cases and the lower temperatures the Strouhal

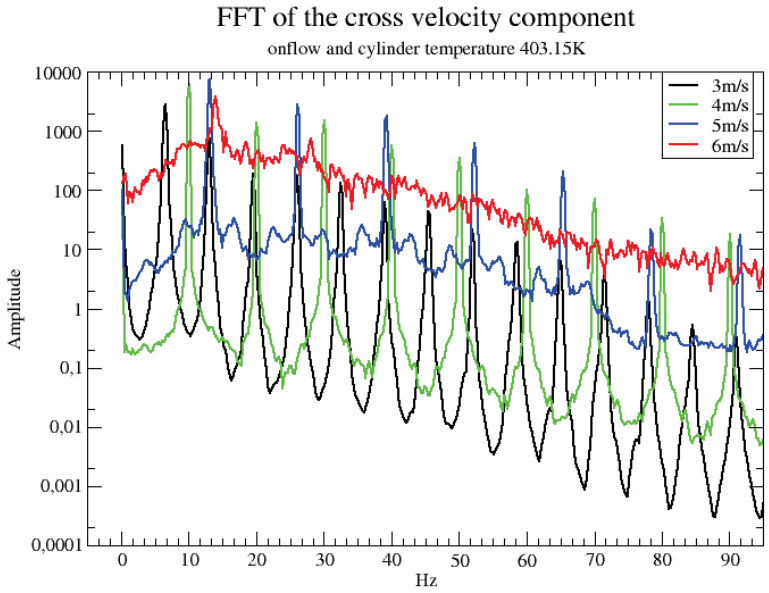

Fig. 3 FFT analysis for the cold cylinder flow with all four onflow velocities

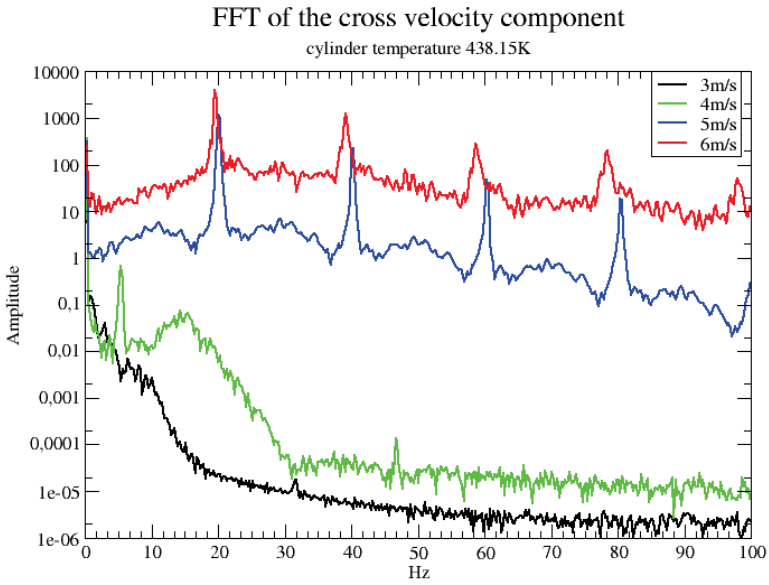

Fig. 4 FFT analysis for the heated (438 K) cylinder flow with all four onflow velocities

number starts in the range of newtonian fluids. Only the highest Reynolds number case has a significant lower Strouhal number. Furthermore three flow cases reveal that for a critical temperature the vortex shedding process stops and the a stable separation bubble exists. Interestingly one flow case is different to the other cases, the flow topologies for the Reynolds number of 44 seem to be less sensitive to the change of the cylinder wall temperatures. Over the whole temperature range the vortex shedding flow structure is observable whilst the other flow cases show crucial damping effects. An explanation can't be given now, therefore, this point is a topic for further research work.

B. Onflow Velocity and Temperature Dependent Flow Topology

Based on the frequency analysis of the cylinder wake flow, associated flow field visualisations have been performed in oder to relate the FFT results to flow topology and characteristic parameters. This part of the study concentrates on the 4 m/s and 6 m/s onflow case, since these flow cases show the most significant flow phenomena observed during the FFT analysis.

For the visualization of velocity and vortical flow structures the line integration convolution technique (LIC) introduced by Chabral [8] has been applied. These integrated visualization pattern deliver a qualitative impression of the flow but not a quantitative evaluation. In fact, even in regions with very

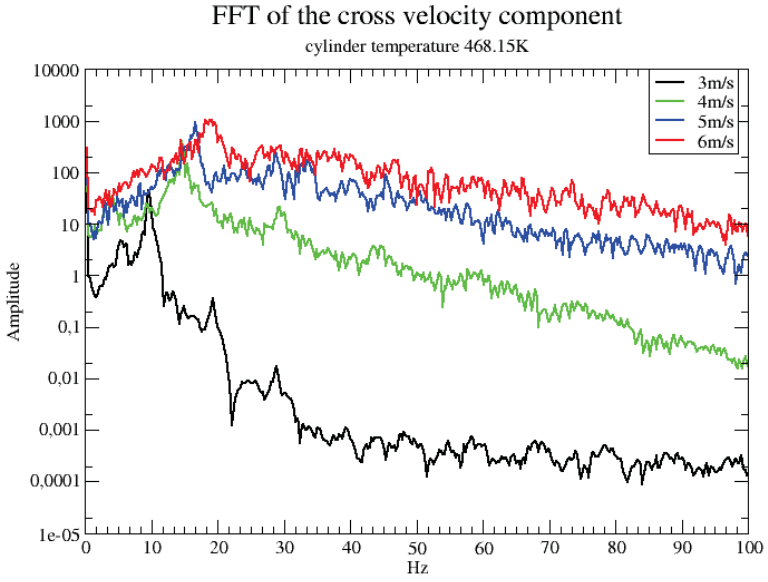

Fig. 5 FFT analysis for the heated (468 K) cylinder flow with all four onflow velocities

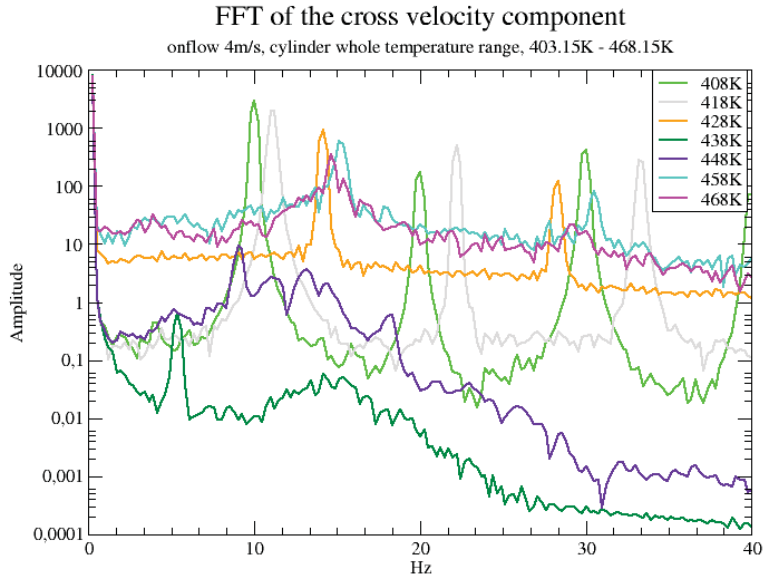

Fig. 6 FFT analysis for the thermal cylinder flow with 4 m/s onflow velocities

small vectorial values, even close to zero, a flow pattern can be integrated and a flow trend can be deduced. However, if the information is too small, then the integration algorithm fails and, as result, at those regions noisy dot pattern are visible. At region with nearly the same velocity some white lines are occurring.

Additionally, the following plots are coloured coded, as colour indicator the local Reynolds number is used, due to the fact that, in case of non-Newtonian fluids, the dynamic viscosity strongly depends on the shear rate. A global Reynolds number is useful for the characterisation of the undisturbed inflow condition. However, a definition of a local Reynolds number,

$$Re\left(\eta(\dot{\gamma})\right) = \frac{\rho\ V_{local}\ D}{\eta(\dot{\gamma})}\,, \tag{5}$$

is meaningful due to the high variation of the shear rates close to viscous walls or in high shearing layers of vortices and its effect on viscosity. The ratio between inertia and viscous forces can drastically change locally and can deviate orders of magnitude from the global Reynolds number. It has to be remarked that at the viscous wall the local Reynolds is zero due to the vanishing velocity, however, in the visualisation process the colour information is interpolated over the whole grid cell, thus in the following figures the zero local Reynolds number band at the wall is not visible due to the narrow band of the thin wall grid cells.

Figs. 10-12 the flow structures are shown for the 4 m/s onflow case. The global comparison of the visible structures are confirming the results of the FFT: the initial vortex shedding process for the reference case is vanishing to a barely

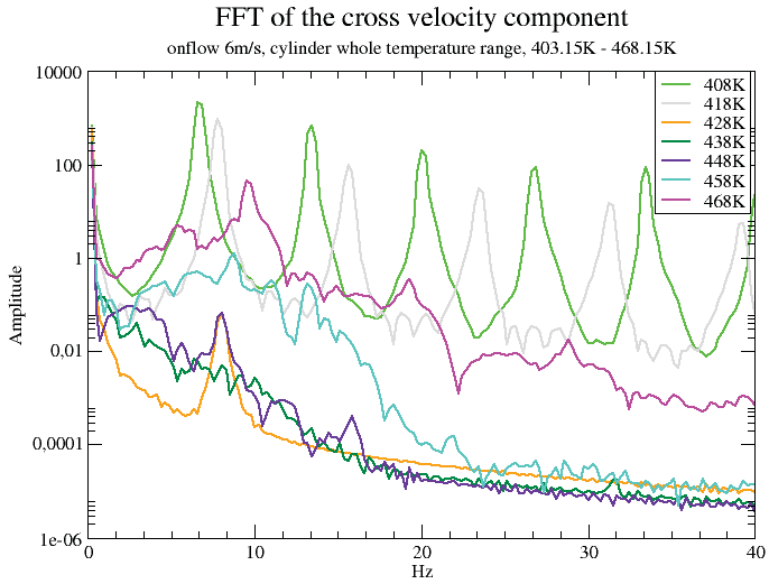

Fig. 7 FFT analysis for the thermal cylinder flow with 6 m/s onflow velocities

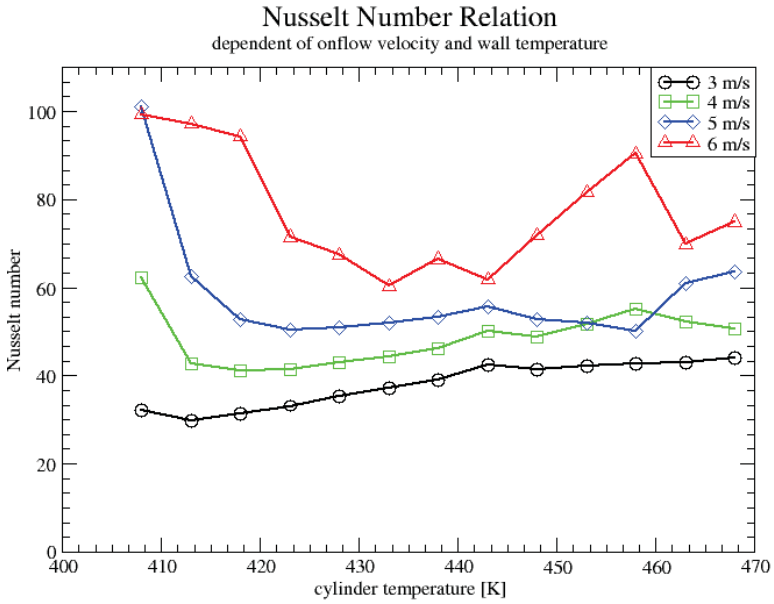

Fig. 8 Nussel number in dependence of onflow velocity and cylinder wall temperature

fluctuating nearly steady separated vortex bubble at 438 K and recovers again at 468 K, though on a lower level of vortex shedding amplitudes.

The local Reynolds number plots are revealing, as expected, a concentration of high shear rates around the cylinder and in highly curved regions of the vortex shedding. Additionally, at spots of higher local Reynolds numbers occur in the wake flow, where the fluid is locally but differentially accelerated.

In principle the flow structures for the 6 m/s onflow case are similar, however the vortex shedding is not vanishing at all, but then more compact.

Figs. 13 and 14 the flow structures are compared for the 4 m/s and 6 m/s onflow case in detail. After the vortex shedding recovering the lower onflow case shows weaker effective Reynolds numbers and more streamdown widespread but a narrower vortex shedding band in the cylinder wake which coresponds to the higher dominant frequency in the FFT results. The higher onflow case shows high fluctuations and more compact separating vortices close to the cylinder but later in the wake a less compact vortex shedding band with a lower dominant frequency.

The impact of the temperature is evident, therefore, we have a look on another characteristical parameter, the local or effective Prandtl number which is defined as:

$$Pr_{eff} := \frac{\eta_{eff} c_p}{\lambda} . \tag{6}$$

In this equation the local, shear and temperature dependent effective viscosity occurs, the heat capacity c_p and the heat

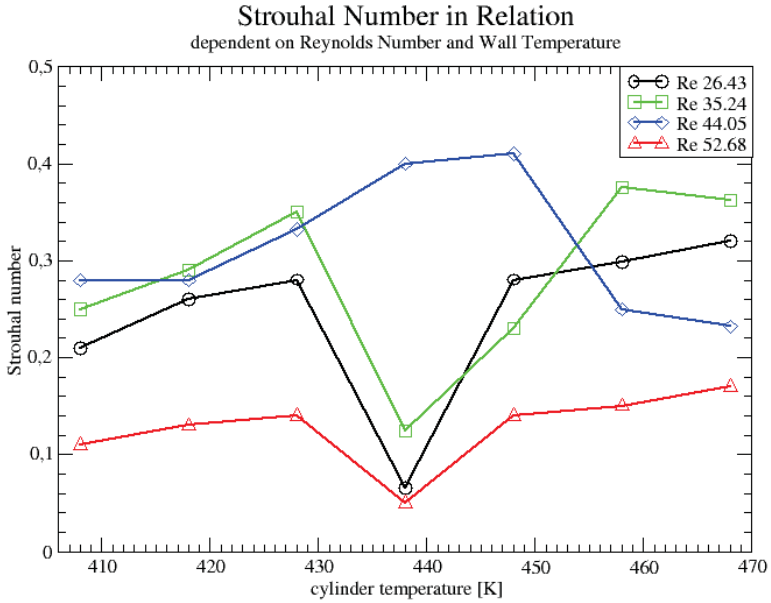

Fig. 9 Strouhal number in dependence of the global Reynolds number and the cylinder wall temperature

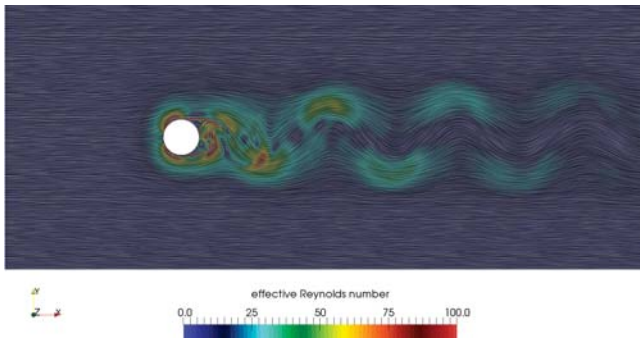

Fig. 10 Local Reynolds number in dependence of the shear rate for the cold cylinder flow with 4 m/s onflow velocity, additionally LIC visualisation of the flow field

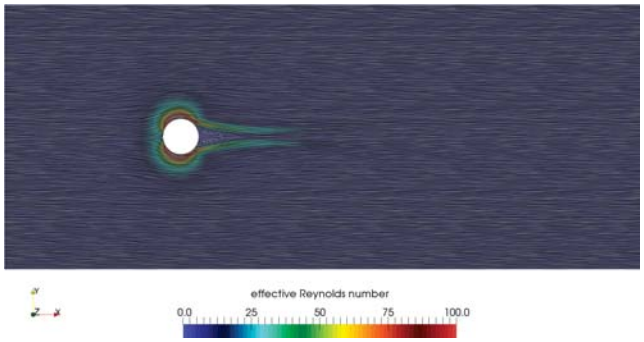

Fig. 11 Local Reynolds number in dependence of the shear rate for the heated cylinder (438 K) flow with 4 m/s onflow velocity, additionally LIC visualisation of the flow field

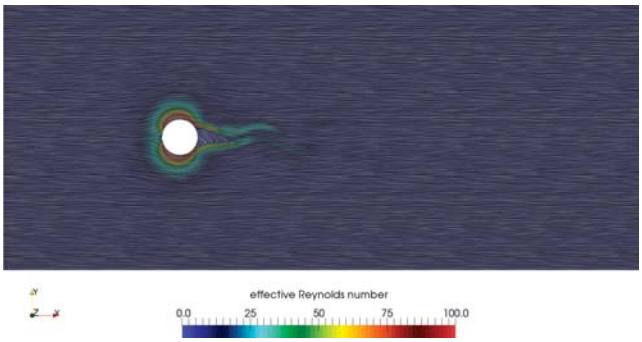

Fig. 12 Local Reynolds number in dependence of the shear rate for the heated cylinder (468 K) flow with 4 m/s onflow velocity, additionally LIC visualisation of the flow field

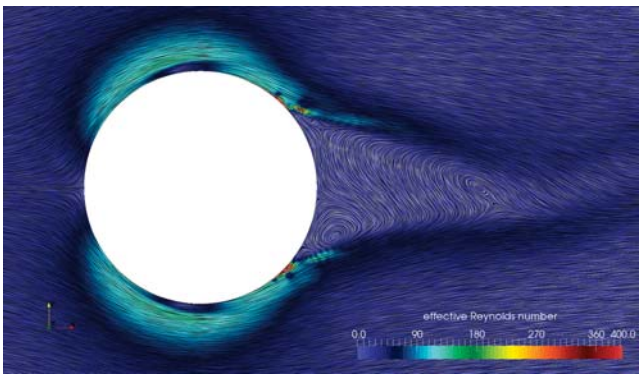

Fig. 13 View on the local Reynolds number close to the heated cylinder (468 K) flow with 4 m/s onflow velocity, additionally LIC visualisation of the flow field

conductivity λ. Since the last two quantities can be assumed as constant, the local Prandtl number reflects the properties of the effective viscosity. Figs. 15 and 16 the colour coded effective Prandt number is compared for the 4 m/s case.

It is remarkable that the effective Prandtl number in the front, upper and lower neighbourhood of the cylinder wall is nearly the same for both cases, they differ slightly at the rear part and distinctly in the wake field. This is a strong indication that instabilities play the significant role for the generation of the temperature and dependent vortex shedding. Therefore, the future research work will focus on

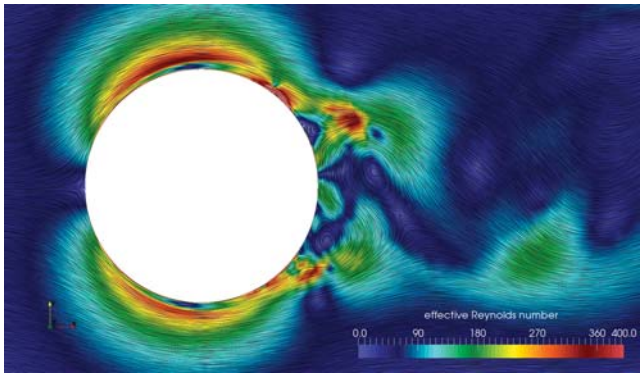

Fig. 14 View on the local Reynolds number close to the heated cylinder (468 K) flow with 6 m/s onflow velocity, additionally LIC visualisation of the flow field

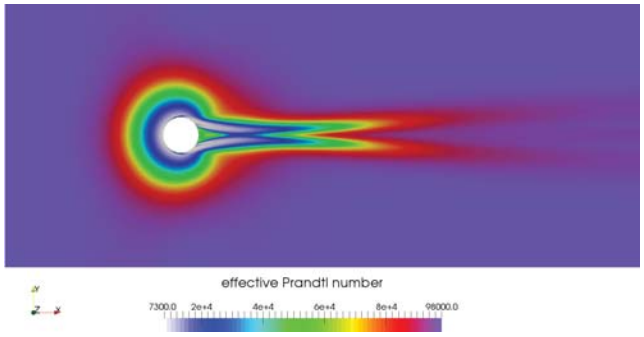

Fig. 15 Effective Prandtl number in dependence of the shear rate for the heated cylinder (438 K) flow with 4 m/s onflow velocity

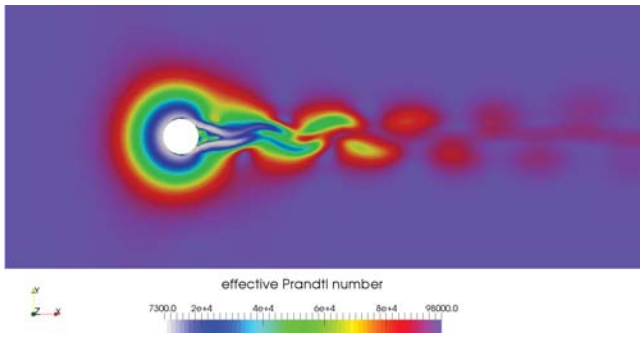

Fig. 16 Effective Prandtl number in dependence of the shear rate for the heated cylinder (468 K) flow with 4 m/s onflow velocity

these instability mechanisms.

IV. Conclusion

In this numerical simulation study the flow of a shear thinning Carreau fluid around a heated cylinder has been investigated. Special attention is paid to the impact of increasing onflow velocity and increasing wall temperature of the cylinder on the flow structure of the wake field. It could be observed that the thermal-viscous behaviour of the Carreau fluid leads to the interesting effects that with increasing cylinder temperature a former Kármán vortex street like wake field is damped and a stable separation bubble establishes. With further increase of the wall temperature the typical vortex shedding flow structure recovers again. It could also shown that this process is associated with first an increase of the dominant vortex shedding related frequencies, a vanishing of typical vortex shedding oscillations and a new appearance of lower vortex shedding frequencies but with significantly lower amplitudes. The analysis of the effective Prandtl number plots has shown that instabilities may cause these uncommon behaviour.

Interestingly one flow case is different then the other, the flow topologies for the Reynolds number of 44 seem to be less sensitive to the change of the cylinder wall temperature. Over the whole temperature range a vortex shedding is observable whilst the other flow cases show significant damping effects preventing a vortex shedding. An explanation can't be given now, thus this point is a topic for further research work.

Acknowledgment

The authors would like to thank the German Aerospace Center (DLR) and the University of Kassel for greatly supporting this research work.

References

[1] Andrade, E. N. D.: A theory of the viscosity of liquids. part 1. Philosophical Magazine, Vol. 17, pp. 497-511, 1934.
[2] CentaurSoftware, http://www.centaursoft.com.
[3] Bird, R. B.: Non-Newtonian behavior of polymeric liquids. Physica A: Statistical and Theoretical Physics, Vol. 118, No. 1-3, pp. 3-16, 1983.
[4] Bird, R. B., Curtiss, C. F.: Nonisothermal polymeric fluids. Rheol. Acta, 35:103109, 1983.
[5] Bird, R. B., Hassager, O.: Dynamics of Polymeric Liquids: Vol.1: Fluid Mechanics. Series: Dynamics of Polymeric Liquids, London, New York, John Wiley & Sons, 1987.
[6] Bognár, G., Kovács, J.: Non-isothermal steady flow of power-law fluids between parallel plates. International Journal of Mathematical Models and Methods in Applied Science, 6(1), 2012.
[7] Carreau, P. J.: Rheological equations from molecular network theories. J. Rheol., Vol. 16, No. 1, pp. 99-127, 1972.
[8] Chabral, B.; Leedom, L. C.: Imaging Vector Fields Using Line Integral Convolution. In: Proceedings of SIGGRAPH 93. pp. 263-270, New York, 1993.
[9] Coelho, P. M.; Pinho, F. T. Vortex shedding in cylinder flow of shear-thinning fluids. II. Flow characteristics. J. Non-Newtonian Fluid Mech. Vol. 110, pp. 177-193, 2003.
[10] Eisenlohr, H., Eckelmann, H.: Vortex splitting and its consequences in the vortex street wake of cylinders at low Reynolds number. Phys. Fluids A 1 (2), pp. 189192, 1989.
[11] Ferry, J. D.: Viscoleastic Properties of Polymers. Third edition, New York; John Wiley & Sons, 1980.
[12] Fey, U., König, M., Eckelmann, H.: A new Strouhal Reynolds number relationship for the circular cylinder in the range 47 ¡ Re ¡ 2 105. Phys. Fluids 10, pp. 15471549, 1998.
[13] von Kármán, Th.: Über den Mechanismus des Widerstandes, den ein bewegter Körper in einer Flüssigkeit erfährt. Nachrichten der K. Gesellschaft der Wissenschaften zu Göttingen, Mathematisch-physikalische Klasse, 1911.
[14] von Kármán, Th., Rubach. H.: Über den Mechanismus des Flüssigkeits- und Luftwiderstandes. Physikalische Zeitschrift, 13, pp. 4959, 1911.
[15] Knopp, T., Zhang, X., Kessler, R. and Lube, G.: Enhancement of an industrial finite-volume code for large-eddy-type simulation of incompressible high Reynolds number flow using near-wall modelling. Journal of Computer Methods in Applied Mechanics and Engineering, Vol. 199, pp. 890-902, 2010.
[16] Monkewitz P. A., Williamson, C. H. K., Miller, G. D.: Phase dynamics of Kármán vortices in cylinder wakes, Phys. Fluids 8, pp. 9196, 1996.
[17] Ostwald, W.: Ueber die rechnerische Darstellung des Strukturgebietes der Viskosität, Kolloid Zeitschrift 47 (2), pp. 176-187, 1929.
[18] Owens, R. G.,Phillips, T. N.: Computational Rheology. Computational Rheology. Imperial College Press, ISBN 9781860941863, 2002.
[19] Skelland, A. H. P.: Non-Newtonian flow and heat transfer. John Wiley & Sons, New York, 1967.

[20] Soares, A. A., Ferreira, J. M., Chhabra, R. P.: Flow and Forced Convection Heat Transfer in Crossflow of Non-Newtonian Fluids over a Circular Cylinder. Ind. Eng. Chem. Res. Vol. 44, pp. 5815-5827, 2003.
[21] Vít, T., Ren, M., Trávníček, Z.,: Maršík, F.: The influence of temperature gradient on the StrouhalReynolds number relationship for water and air. Experimental Thermal and Fluid Science, Vol. 31, pp. 751-760, 2007.
[22] Wang, A.-B. , Trávníček, Z., Chia, K.-C.: On the relationship of effective Reynolds number and Strouhal number for the laminar vortex shedding of a heated circular cylinder. Phys. Fluids 12 (6), pp. 1401-1410, 2000.
[23] Wendt, J. F. (Ed.): Computational Fluid Dynamics - An Introduction. Third edition, Berlin, Heidelberg; Springer, 2009.
[24] Williams, M. L., Landel, R. F., Ferry, J. D: The Temperature Dependence of Relaxation Mechanisms in Amorphous Polymers and Other Glass-forming Liquids. Journal of the American Chemical Society, Vol. 77, pp. 3701-3707, 1955.
[25] Williamson, C. H. K.: Vortex dynamics in the cylinder wake, Ann. Rev. Fluid. Mech. 28, pp. 477539, 1996.

Markus Rütten is research scientist at the German Aerosapce Center at Göttingen, his reasearch fields are vortical flows, turbulence and non-Newtonian thermo viscous shear thinning fluids.

Olaf Wünsch is Professor at the University of Kassel, head of the Fluid Dynamics Group in the Department of Mechanical Engineering. His professions are non-Newtonian fluids, in particular visco-elastic fluids, bio-medical flows, fluid-structure interaction and dynamical systems.